



Since January 2020 Elsevier has created a COVID-19 resource centre with free information in English and Mandarin on the novel coronavirus COVID-19. The COVID-19 resource centre is hosted on Elsevier Connect, the company's public news and information website.

Elsevier hereby grants permission to make all its COVID-19-related research that is available on the COVID-19 resource centre - including this research content - immediately available in PubMed Central and other publicly funded repositories, such as the WHO COVID database with rights for unrestricted research re-use and analyses in any form or by any means with acknowledgement of the original source. These permissions are granted for free by Elsevier for as long as the COVID-19 resource centre remains active.



## Original Article

## Stability of SARS-CoV-2 and influenza virus varies across different paper types



Ryohei Hirose<sup>a,b,\*</sup>, Hajime Miyazaki<sup>a</sup>, Risa Bandou<sup>a,c</sup>, Naoto Watanabe<sup>a,b</sup>, Takuma Yoshida<sup>a,b</sup>, Tomo Daidoji<sup>a</sup>, Yoshito Itoh<sup>a</sup>, Takaaki Nakaya<sup>a</sup>

<sup>a</sup> Department of Infectious Diseases, Graduate School of Medical Science, Kyoto Prefectural University of Medicine, 465 Kajii-cho, Kawaramachi-Hirokoji, Kamigyo-ku, Kyoto, 602-8566, Japan

<sup>b</sup> Department of Molecular Gastroenterology and Hepatology, Graduate School of Medical Science, Kyoto Prefectural University of Medicine, 465 Kajii-cho, Kawaramachi-Hirokoji, Kamigyo-ku, Kyoto, 602-8566, Japan

<sup>c</sup> Department of Forensics Medicine, Graduate School of Medical Science, Kyoto Prefectural University of Medicine, 465 Kajii-cho, Kawaramachi-Hirokoji, Kamigyo-ku, Kyoto, 602-8566, Japan

## ARTICLE INFO

**Keywords:**  
SARS-CoV-2  
Paper  
Stability  
Influenza A virus  
Postcard

## ABSTRACT

**Introduction:** The assessment of the risk of virus transmission through papers, such as postcards, is important. However, the stability of severe acute respiratory syndrome coronavirus 2 (SARS-CoV-2) and influenza A virus (IAV) on different types of papers is currently unknown. Investigation of the survival time of these viruses on different types of papers will provide insights into their risk of long-distance transport by postal items.

**Methods:** We evaluated the stability of SARS-CoV-2 and IAV, mixed with a culture medium, on the surface of postcards with various coatings, including plain paper (PP), inkjet paper (IP), and inkjet photo paper (IPP). The surface structure of each paper was microscopically assessed.

**Results:** The surface structures of PP, IP, and IPP varied greatly depending on the presence or absence, and type, of coat layer, regardless of the base material. IP and IPP surfaces were less conducive to virus survival than PP surfaces, because of the difference in surface shapes. The survival times of SARS-CoV-2 on each paper were approximately 59.8 (PP), 6.5 (IP), and 9.8 h (IPP), and significantly longer than those of IAV (10.3, 1.8, and 3.3 h, respectively).

**Conclusions:** The risk of SARS-CoV-2 transmission via paper, such as postcards, is significantly higher than that of IAV transmission. While PP, IP, and IPP have the same base material, their surface structures differ, which affects viral stability. The IP and IPP surfaces are less suitable for virus survival. This study provides novel insights into the risks of viral transmission via paper.

## 1. Introduction

Recently, the stability of severe acute respiratory syndrome coronavirus 2 (SARS-CoV-2) on various surfaces has been reported, providing information for infection control [1–3]. Moreover, several studies have reported that coronaviruses are relatively more stable than certain enveloped viruses, such as influenza A virus (IAV) [3–8].

The stability of SARS-CoV-2 on the surface of cardboard and printing paper is reportedly lower than that on the surface of stainless steel and

plastic [1,2,9]. Specifically, SARS-CoV-2 is completely inactivated within 3 h on printing paper surface, but is not completely inactivated on the surface of banknote paper and cardboard, even after 24 h. Although the stability of SARS-CoV-2 on the surface of various papers can vary significantly, the stability of SARS-CoV-2 on paper with different surface structures remains to be investigated.

Investigation of the survival time of viruses on different paper types will provide insights into the risk of the long-distance transport of viruses by postal items, such as postcards. In this study, we evaluated and

; SARS-CoV-2, severe acute respiratory syndrome coronavirus 2; IAV, influenza A virus; PP, plain paper; IP, inkjet paper; IPP, inkjet photo paper; MDCK, Madin–Darby canine kidney; DMEM, Dulbecco's modified Eagle's medium; FBS, fetal bovine serum; PBS, phosphate-buffered saline; TCID<sub>50</sub>, 50% tissue culture infectious dose; FFU, focus-forming units.

\* Corresponding author. Department of Infectious Diseases, Graduate School of Medical Science, Kyoto Prefectural University of Medicine, 465 Kajii-cho, Kawaramachi-Hirokoji, Kamigyo-ku, Kyoto, 602-8566, Japan.

E-mail address: [ryo-hiro@koto.kpu-m.ac.jp](mailto:ryo-hiro@koto.kpu-m.ac.jp) (R. Hirose).

<https://doi.org/10.1016/j.jiac.2021.11.006>

Received 15 July 2021; Received in revised form 14 October 2021; Accepted 9 November 2021

Available online 13 November 2021

1341-321X/© 2021 Japanese Society of Chemotherapy and The Japanese Association for Infectious Diseases. Published by Elsevier Ltd. All rights reserved.

**Table 1**

The virus recovery efficiency on each paper.

	Virus recovery efficiency (mean $\pm$ standard error)		
	PP	IP	IPP
SARS-CoV-2	59.7 $\pm$ 16.9%	69.5 $\pm$ 19.5%	59.7 $\pm$ 16.9%
IAV	58.8 $\pm$ 6.5%	60.0 $\pm$ 6.1%	60.0 $\pm$ 3.5%

compared the stability of SARS-CoV-2 and IAV, mixed with a culture medium, on the surface of postcards with various coatings, including plain paper (PP), inkjet paper (IP), and inkjet photo paper (IPP). The three-dimensional surface structure of each paper was microscopically assessed, and the rate of viral droplet drying was determined.

## 2. Materials and methods

### 2.1. Viruses and cells

Madin–Darby canine kidney (MDCK) cells were purchased from the RIKEN BioResource Center Cell Bank (Ibaragi, Japan) and cultured in minimal essential medium (Sigma, St Louis, MO, USA) supplemented with 10% fetal bovine serum (FBS) and standard antibiotics (penicillin/streptomycin). IAV (clinical strain H3N2 isolated in 2012) was cultured in MDCK cells and stored at  $-80^{\circ}\text{C}$ . Viral titers were determined in terms of focus-forming units (FFU) in MDCK cells [10].

VeroE6/TMPRSS2 cells, expressing the transmembrane serine protease TMPRSS2, were purchased from the Japanese Collection of Research Bioresources Cell Bank (Osaka, Japan) and cultured in Dulbecco's modified Eagle's medium (DMEM; Sigma) supplemented with 5% FBS and G418 (Nacalai Tesque, Kyoto, Japan) [11]. SARS-CoV-2 (JPN/TY/WK-521) was generously provided by the National Institute of Infectious Diseases (Tokyo, Japan). The virus was cultured in VeroE6/TMPRSS2 cells and stored at  $-80^{\circ}\text{C}$ . Viral titers were measured in terms of 50% tissue culture infectious dose (TCID<sub>50</sub>) in

VeroE6/TMPRSS2 cells.

Cellular debris, culture medium, FBS, and other chemical substances were removed from the solution containing the viruses cultured in the cells. Specifically, both viruses were concentrated and purified as follows: 96 h post infection, the culture medium was harvested and centrifuged for 10 min at  $2500\times g$  at  $4^{\circ}\text{C}$  to eliminate cellular debris. Virions in the supernatant were sedimented using 20% (w/w) sucrose cushion in phosphate-buffered saline (PBS; Nacalai Tesque) through ultracentrifugation at 27,000 rpm for 2.5 h at  $4^{\circ}\text{C}$  in a Beckman SW28 rotor, and the sedimented virions were recovered using PBS without additives [12].

### 2.2. Surface shape observation

The surfaces of PP, IP, and IPP were viewed with optical (VHX-7000, Keyence, Osaka, Japan) and laser scanning (VK-9510, Keyence) microscopes.

### 2.3. Complete drying time measurement

The time required for 2  $\mu\text{L}$  of DMEM to completely dry and solidify on the surface of each paper type was measured [13]. In an indoor environment (temperature  $25^{\circ}\text{C}$ , humidity 40%), 2  $\mu\text{L}$  of each sample was placed on PP, IP, or IPP and weighed over time with an analytical balance (XFR-135, SHINKO DENSHI, Tokyo, Japan). The weight gradually decreased as the sample dried, and the time the weight ceased to decrease was defined as the "complete drying time."

### 2.4. Evaluation of viral stability on various paper surfaces

The survival duration of the viruses was assessed on the surfaces of PP, IP, and IPP. IAV or SARS-CoV-2 was mixed with DMEM containing no additives and applied in 2- $\mu\text{L}$  aliquots to each surface (amount of virus:  $2.0 \times 10^5$  FFUs or  $2.0 \times 10^5$  TCID<sub>50</sub>, respectively). Each sample

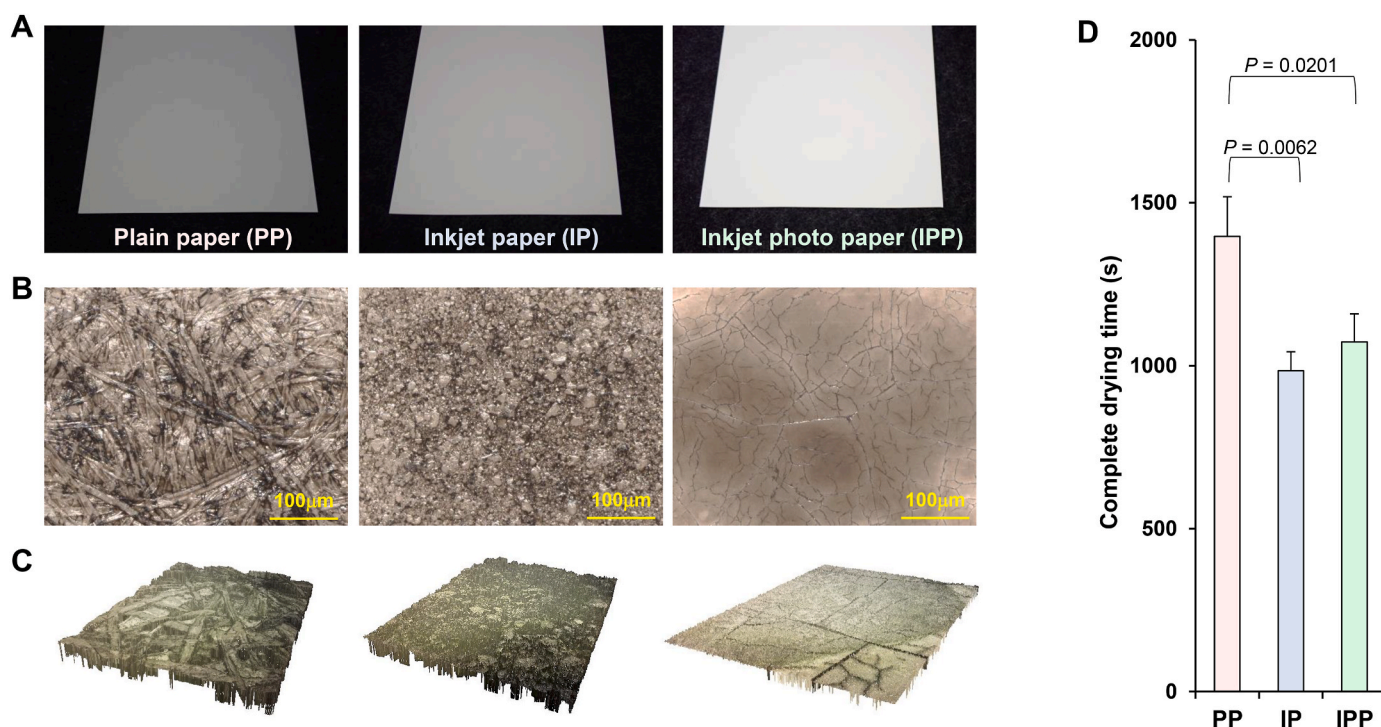


**Fig. 1.** Surface shape observation and complete drying time analysis. (A) Appearance of plain paper (PP), inkjet paper (IP), and inkjet photo paper (IPP). (B) The surface shapes of PP, IP, and IPP were observed using an optical microscope (VHX-7000, Keyence, Osaka, Japan). (C) The three-dimensional surface shapes of PP, IP, and IPP were observed using an optical microscope (VHX-7000, Keyence, Osaka, Japan) and a laser scanning microscope (VK-9510, Keyence). (D) Time required for 2  $\mu\text{L}$  of Dulbecco's modified Eagle's medium on the surface of each paper (PP, IP, and IPP) to completely dry (complete drying time).

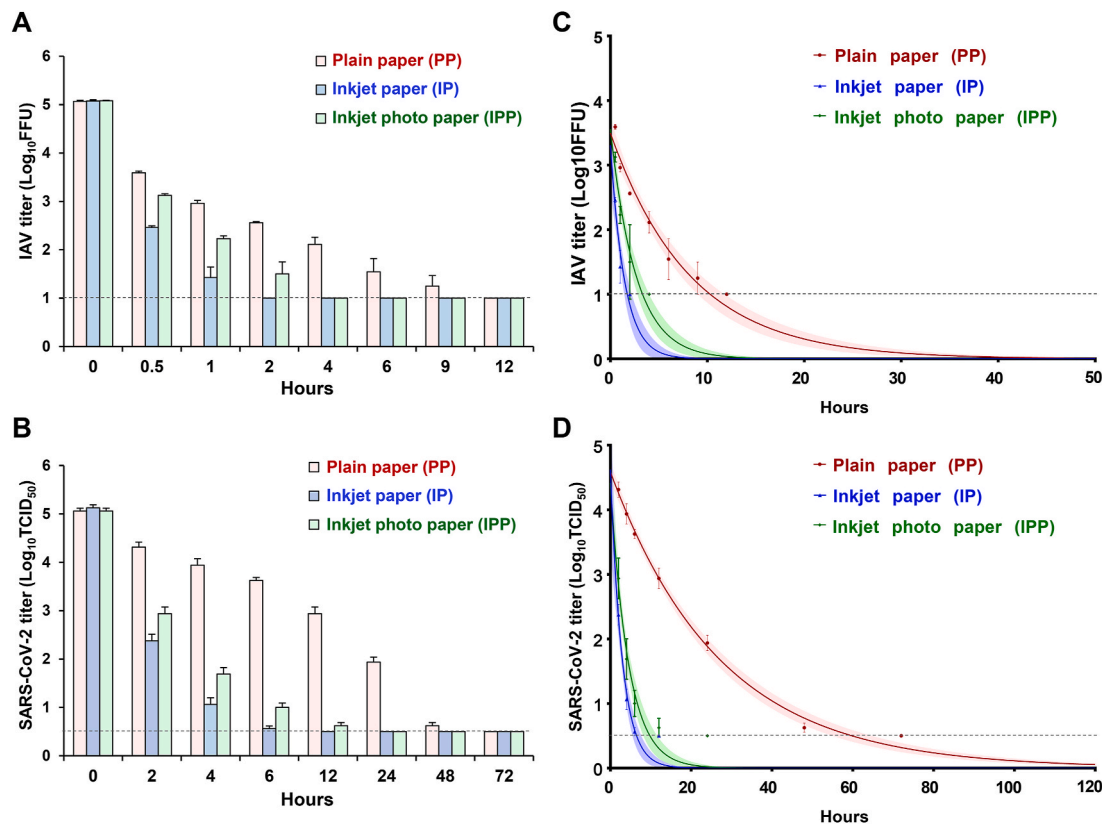


**Fig. 2.** (A, B) Fluctuations in the titer of influenza A virus (IAV) and severe acute respiratory syndrome coronavirus 2 (SARS-CoV-2) surviving on the surface of PP, IP, and IPP. For each measurement, four independent experiments were performed, and the results are expressed as mean ± standard error. (C, D) Stability of IAV and SARS-CoV-2 on the surface of PP, IP, and IPP. Data were analyzed using GraphPad Prism 7 software (GraphPad, Inc., La Jolla, CA, USA). The elapsed time was defined as an explanatory variable (X-axis), and the log virus titer of IAV or SARS-CoV-2 was defined as an explained variable (Y-axis); least-squares linear regression analysis with a logarithmic link function was performed for each virus, to generate a curve of regression. The upper and lower confidence limits are represented by dotted curves. The black dotted straight lines represent the detection limit titers of IAV and SARS-CoV-2.

**Table 2**  
Survival time of viruses on each surface.

	Survival time, hour, median (95% CI)	
	IAV	SARS-CoV-2
Plain paper (PP)	10.29 (8.80–12.06)	59.78 (53.99–65.57)
Inkjet paper (IP)	1.75 (1.38–2.32)	6.48 (5.30–7.88)
Inkjet photo paper (IPP)	3.32 (2.69–4.15)	9.78 (7.88–11.92)

The elapsed time was defined as an explanatory variable (X-axis), and the log virus titer of IAV or SARS-CoV-2 was defined as an explained variable (Y-axis). Least-squares linear regression analysis was performed for each virus to generate a curve of regression. The measurement limits of the titers of IAV and SARS-CoV-2 were 10<sup>1</sup> FFU and 10<sup>0.5</sup> TCID<sub>50</sub>, respectively; therefore, the survival times of IAV and SARS-CoV-2 were defined as the X values when the Y values of the regression curves were 1.0 and 0.5, respectively.

was incubated in a controlled environment (25 °C and 40%–50% humidity) for 0–72 h; thereafter, the residual virus on the surface was recovered in 1 mL of DMEM and titrated [3,6]. For each measurement, four independent experiments were performed, and the results were expressed as mean ± standard error of the mean. Zero-hour incubation refers to virus recovery immediately after applying the virus mixture to each surface.

When the virus solution was applied to the surface of each paper, it penetrated a little deeper into the paper, but did not reach the back of

the paper. The virus remaining on the paper surface after incubation was eluted and collected by immersing the paper in DMEM for 15 min. Additionally, before the evaluation, we confirmed that the virus recovery efficiency on each paper was approximately comparable (Table 1).

### 2.5. Statistical analysis

Data were analyzed using GraphPad Prism 7 software (GraphPad, Inc., La Jolla, CA, USA). The elapsed time was defined as an explanatory variable (X-axis), and the log virus titer of IAV or SARS-CoV-2 was defined as an explained variable (Y-axis). Least-squares linear regression analysis was performed for each virus to generate a regression curve. The measurement limits of the titers of IAV and SARS-CoV-2 were 10<sup>1</sup> FFU and 10<sup>0.5</sup> TCID<sub>50</sub>, respectively; the survival times of IAV and SARS-CoV-2 were defined as the X value when the Y value of the regression curves were 1.0 and 0.5, respectively. The half-life of the virus changed depending on the elapsed time or the amount of virus remaining on each surface. The half-life of IAV and SARS-CoV-2 was calculated from the slope of each regression curve when the amount of virus remaining on the surface was 2, 3, and 4 Log<sub>10</sub>FFU or Log<sub>10</sub>TCID<sub>50</sub>, respectively [3, 14]. Furthermore, Pearson’s correlation coefficient was used to assess the correlation between the survival time and the complete drying time.

## 3. Results

The surfaces of PP, IP, and IPP were viewed using microscopes. Paper surface analysis revealed that PP, IP, and IPP had very different surface structures (Fig. 1A–C). The time required for 2 μL of DMEM to

**Table 3**  
Half-life of viruses on each surface.

	Half-life, hour, median (95% CI)					
	IAV			SARS-CoV-2		
	4 (Log <sub>10</sub> FFU)	3 (Log <sub>10</sub> FFU)	2 (Log <sub>10</sub> FFU)	4 (Log <sub>10</sub> TCID <sub>50</sub> )	3 (Log <sub>10</sub> TCID <sub>50</sub> )	2 (Log <sub>10</sub> TCID <sub>50</sub> )
Plain paper (PP)	0.62 (0.51–0.77)	0.82 (0.68–1.02)	1.24 (1.02–1.53)	2.03 (1.82–2.27)	2.71 (2.42–3.02)	4.06 (3.64–4.53)
Inkjet paper (IP)	0.11 (0.07–0.19)	0.15 (0.09–0.25)	0.22 (0.14–0.38)	0.22 (0.15–0.33)	0.29 (0.20–0.44)	0.44 (0.30–0.67)
Inkjet photo paper (IPP)	0.20 (0.14–0.28)	0.26 (0.19–0.37)	0.39 (0.29–0.56)	0.39 (0.24–0.51)	0.45 (0.32–0.68)	0.68 (0.48–1.02)

The elapsed time was defined as an explanatory variable (X-axis), and the log virus titer of IAV or SARS-CoV-2 was defined as an explained variable (Y-axis). A linear regression analysis with logarithmic link function was performed for each virus to create a curve of regression. The half-life of the virus changed depending on the elapsed time or the amount of virus remaining on each surface. Therefore, the half-life of each virus was calculated from the slope of each regression curve when the amount of virus remaining on the surface was 2, 3, and 4 Log<sub>10</sub>FFU or Log<sub>10</sub>TCID<sub>50</sub> respectively.

completely dry on the surface of each paper type was measured. The time taken for complete drying of DMEM on the surface of PP was significantly longer than that on IP and IPP (Fig. 1D).

The stability of SARS-CoV-2 and IAV, mixed with DMEM, was evaluated on the surface of PP, IP, and IPP. SARS-CoV-2 and IAV were more rapidly inactivated on IP and IPP than on PP (Fig. 2). IAV on the surface of PP, IP, and IPP was inactivated within 12, 2, and 4 h, respectively, and SARS-CoV-2 was inactivated within 72, 12, and 24 h, respectively.

The survival times of SARS-CoV-2 and IAV were significantly shorter on IP and IPP than on PP, and were significantly shorter on IP than on IPP. The survival time of SARS-CoV-2 on PP was approximately six-fold longer than that of IAV, and the survival time of SARS-CoV-2 on IP and IPP was approximately three-fold longer than that of IAV, demonstrating that SARS-CoV-2 was more stable than IAV (Fig. 2 and Table 2). The survival time of SARS-CoV-2 and IAV positively correlated with the complete drying time, with a correlation coefficient of 0.981 for SARS-CoV-2 and 0.858 for IAV ( $P < 0.001$ ).

The half-lives of SARS-CoV-2 and IAV were significantly shorter on IP and IPP than on PP. The half-life of SARS-CoV-2 on PP was approximately three-fold longer than that of IAV, and the half-life of SARS-CoV-2 on IP and IPP was approximately two-fold longer than that of IAV (Table 3). These half-life comparisons showed the same trend, regardless of the amount of virus remaining on the surface.

#### 4. Discussion

It is important to assess the risk of viral transmission via mail because of the potential widespread impact. Here, we analyzed PP, IP, and IPP, which are papers typically used for postcards. To prevent ink bleeding, IP and IPP are treated to allow rapid drying of the surface. Surface structure analysis showed that PP, IP, and IPP have different properties. We confirmed that the surface structures of PP, IP, and IPP vary greatly depending on the presence or absence and type of coat layer, regardless of the base material. DMEM dried significantly faster on the surface of IP and IPP than on that of PP. Differences in porosity and ease of drying influence virus stability [1–5,15]. Therefore, in this study, we hypothesized that the stability of the virus on the surface of each paper (PP, IP and IPP) might be different.

In our previous study, in which the evaluation conditions such as temperature and humidity were almost the same as in this study, the survival times of SARS-CoV-2 and IAV on stainless steel and glass surfaces were 84.3 and 85.7 h, respectively, and the survival times of IAV on stainless steel and glass surfaces were 11.6 and 10.6 h, respectively [3]. The survival times of SARS-CoV-2 and IAV on PP surfaces were not considerably different from that on stainless steel and glass surfaces. This suggested a relatively high risk of contact transmission through PP. The assessment of virus stability on each paper surface showed that SARS-CoV-2 and IAV were inactivated more quickly on IP and IPP than on PP. Therefore, the surfaces of IP and IPP are less suitable for virus

survival; IP and IPP have a lower risk of viral transmission and can be used relatively safely during SARS-CoV-2 and IAV epidemics. The virus survival time positively correlated with the complete drying time. Therefore, surface treatments that enable the rapid evaporation of surface liquid might reduce the stability of these viruses and contribute to future advances in infection control.

Here, the survival and half-life of SARS-CoV-2 were significantly longer than that of IAV, across different paper types. SARS-CoV-2 is more stable than IAV, which is generally consistent with our results [3–5]. Therefore, SARS-CoV-2 has a higher risk of transmission through paper, such as postcards, than IAV.

Viral titer in the upper respiratory tract-derived body fluid of patients infected with IAV and SARS-CoV-2 ranged from  $1.0 \times 10^2$  to  $2.0 \times 10^6$  FFUs/mL or TCID<sub>50</sub>/mL [16–19]. When 10–100  $\mu$ L of the infectious body fluid is deposited on a paper surface, the maximum absolute viral titer on the paper surface is approximately  $2.0 \times 10^5$  FFUs or TCID<sub>50</sub>. Therefore, in this study, we evaluated the viral stability considering that the virus adhered to the paper surface at  $2.0 \times 10^5$  FFUs or TCID<sub>50</sub>. Therefore, the survival times given in Table 2 are assumed to be close to the maximum values. If the amount of virus adhering to the paper surface is less, the survival time could be shorter than that obtained in this study. SARS-CoV-2 can survive on PP for up to 60 h; therefore, the transmission of SARS-CoV-2 from the sender to the postal worker and from the postal worker to the recipient should be considered. In the case of express delivery, with a duration of approximately 1–2 days, it may be necessary to consider the direct transmission of SARS-CoV-2 from the sender to the recipient. However, thorough infection control within the post office can greatly reduce these concerns, and switching the paper used for postcards from PP to IP or IPP might also reduce the transmission risk.

However, substantial decrease in the amount of virus adhering to the postcards or significant deviations from the environmental conditions of this study (temperature 25 °C, humidity 40%) could change the above considerations/recommendations. Moreover, the mechanism by which surface structure affects virus stability remains unknown. In addition, the coat layer contains water-soluble resins, such as polyethylene oxide and inorganic pigments, such as silica. These chemical substances could shorten the survival time of the virus. Future investigations under various environmental conditions and investigations to elucidate the transmission mechanism are warranted.

#### 5. Conclusions

The risk of SARS-CoV-2 transmission through paper, such as postcards, is significantly higher than that of IAV transmission. IP and IPP surfaces are less suitable for virus survival than PP surfaces; therefore, switching from PP to IP or IPP could reduce the viral transmission risks through paper. This study provides novel insights into viral transmission risks through paper.

## Authorship statement

All authors meet the following ICMJE authorship criteria: (1) the conception and design of the study, or acquisition of data, or analysis and interpretation of data, (2) drafting the article or revising it critically for important intellectual content, and (3) final approval of the version to be submitted.

## Author contributions

Study concept and design: RH. Data acquisition: RH, HM, NW, TY, RB, TD. Data analysis and interpretation: RH, HM, YI and TN. Drafting of the manuscript: RH. Statistical analysis: RH. Secured funding: RH. Administrative/technical/material support: RH. Study supervision: RH and TN.

## Declaration of competing interest

The authors declare no competing financial interests.

## Acknowledgments

We thank Statista, Inc. for assistance in statistical analysis, and thank Editage ([www.editage.com](http://www.editage.com)) for English language editing. This research was supported by Adaptable and Seamless Technology Transfer Program through Target-driven R&D (ASTEP) from the Japan Science and Technology Agency (JST) [grant number JPMJTR21UE and JPMJTM20PR]; the Japan Agency for Medical Research and Development (AMED) (grant number JP 20fk0108077) and JSPS KAKENHI (grant number 21K16326); and Takeda Science Foundation, and Mit-subishi Foundation.

## References

- [1] van Doremalen N, Bushmaker T, Morris DH, Holbrook MG, Gamble A, Williamson BN, et al. Aerosol and surface stability of SARS-CoV-2 as compared with SARS-CoV-1. *N Engl J Med* 2020;382(16):1564–7.
- [2] Chin AWH, Chu JTS, Perera MRA, Hui KPY, Yen HL, Chan MCW, et al. Stability of SARS-CoV-2 in different environmental conditions. *Lancet Microbe* 2020;1(1):e10.
- [3] Hirose R, Ikegaya H, Naito Y, Watanabe N, Yoshida T, Bandou R, et al. Survival of SARS-CoV-2 and influenza virus on the human skin: importance of hand hygiene in COVID-19. *Clin Infect Dis* 2020 [epub ahead of print].
- [4] Kampf G, Todt D, Pfaender S, Steinmann E. Persistence of coronaviruses on inanimate surfaces and their inactivation with biocidal agents. *J Hosp Infect* 2020; 104(3):246–51.
- [5] Otter JA, Donskey C, Yezli S, Douthwaite S, Goldenberg SD, Weber DJ. Transmission of SARS and MERS coronaviruses and influenza virus in healthcare settings: the possible role of dry surface contamination. *J Hosp Infect* 2016;92(3): 235–50.
- [6] van Doremalen N, Bushmaker T, Munster VJ. Stability of Middle East respiratory syndrome coronavirus (MERS-CoV) under different environmental conditions. *Euro Surveill* 2013;18(38):20590.
- [7] Duan SM, Zhao XS, Wen RF, Huang JJ, Pi GH, Zhang SX, et al. Stability of SARS coronavirus in human specimens and environment and its sensitivity to heating and UV irradiation. *Biomed Environ Sci* : BES 2003;16(3):246–55.
- [8] Weber TP, Stilianakis NI. Inactivation of influenza A viruses in the environment and modes of transmission: a critical review. *J Infect* 2008;57(5):361–73.
- [9] Harbourt DE, Haddow AD, Piper AE, Bloomfield H, Kearney BJ, Fetterer D, et al. Modeling the stability of severe acute respiratory syndrome coronavirus 2 (SARS-CoV-2) on skin, currency, and clothing. *PLoS Neglected Trop Dis* 2020;14(11): e0008831.
- [10] Hirose R, Nakaya T, Naito Y, Daidoji T, Watanabe Y, Yasuda H, et al. Mechanism of human influenza virus RNA persistence and virion survival in feces: mucus protects virions from acid and digestive juices. *J Infect Dis* 2017;216(1):105–9.
- [11] Matsuyama S, Nao N, Shirato K, Kawase M, Saito S, Takayama I, et al. Enhanced isolation of SARS-CoV-2 by TMPRSS2-expressing cells. *Proc. Natl. Acad. Sci. U. S. A.* 2020;117(13):7001–3.
- [12] Bárcena M, Oostergetel GT, Bartelink W, Faas FG, Verkleij A, Rottier PJ, et al. Cryo-electron tomography of mouse hepatitis virus: insights into the structure of the coronavirus. *Proc. Natl. Acad. Sci. U. S. A.* 2009;106(2):582–7.
- [13] Hirose R, Nakaya T, Naito Y, Daidoji T, Bandou R, Inoue K, et al. Situations leading to reduced effectiveness of current hand hygiene against infectious mucus from influenza virus-infected patients. *mSphere* 2019;4(5). e00474-19.
- [14] Hirose R, Ikegaya H, Naito Y, Watanabe N, Yoshida T, Bandou R, et al. Reply to gracely. *Clin Infect Dis* 2021;73(3):e854–6.
- [15] Corpet DE. Why does SARS-CoV-2 survive longer on plastic than on paper? *Med Hypothesis* 2021;146:110429.
- [16] Ng EK, Cheng PK, Ng AY, Hoang TL, Lim WW. Influenza A H5N1 detection. *Emerg Infect Dis* 2005;11(8):1303–5.
- [17] Branche AR, Walsh EE, Formica MA, Falsey AR. Detection of respiratory viruses in sputum from adults by use of automated multiplex PCR. *J Clin Microbiol* 2014;52 (10):3590–6.
- [18] Hiroi S, Kubota-Koketsu R, Sasaki T, Morikawa S, Motomura K, Nakayama EE, et al. Infectivity assay for detection of SARS-CoV-2 in samples from patients with COVID-19. *J Med Virol* 2021;93(10):5917–23.
- [19] Shchetinin AM, Tsyganova EV, Protsenko DN, Botikov AG, Gushchin V. A case of moderately severe COVID-19 in a healthcare worker in Russia: virus isolation and full genome sequencing. *Cureus* 2021;13(3):e13733.